Neuron, Vol. 37, 801–811, March 6, 2003, Copyright ©2003 by Cell Press

Probing the Intracellular Calcium Sensitivity of Transmitter Release during Synaptic Facilitation

Felix Felmy, Erwin Neher, and Ralf Schneggenburger*
Abteilung Membranbiophysik and
AG Synaptische Dynamik und Modulation
Max-Planck-Institut für Biophysikalische Chemie
Am Fassberg 11
D-37077 Göttingen
Germany

Summary

In nerve terminals, residual Ca^{2+} remaining from previous activity can cause facilitation of transmitter release by a mechanism that is still under debate. Here we show that the intracellular Ca^{2+} sensitivity of transmitter release at the calyx of Held is largely unchanged during facilitation, which leaves an increased microdomain Ca^{2+} signal as a possible mechanism for facilitation. We measured the Ca^{2+} dependencies of facilitation, as well as of transmitter release, to estimate the required increment in microdomain Ca^{2+}. These measurements show that linear summation of residual and microdomain Ca^{2+} accounts for only 30% of the observed facilitation. However, a small degree of supralinearity in the summation of intracellular Ca^{2+} signals, which might be caused by saturation of cytosolic Ca^{2+} buffer(s), is sufficient to explain facilitation at this CNS synapse.

Introduction

Facilitation is an activity-dependent form of synaptic enhancement, which has been observed at neuromuscular and invertebrate synapses (Katz and Miledi, 1968; Stanley, 1986; Kamiya and Zucker, 1994; Vyshedskiy et al., 2000) as well as in the mammalian CNS (Wu and Saggau, 1994; Atluri and Regehr, 1996; Rozov et al., 2001; see Zucker and Regehr, 2002, for a review). During trains of presynaptic action potentials (AP), facilitation builds up and, together with other pre- and postsynaptic factors, determines the synaptic strength and, hence, the information transfer across synapses. It is widely accepted that the elevated intracellular Ca^{2+} concentration ($[Ca^{2+}]_i$) that remains from previous stimuli, termed "residual" $[Ca^{2+}]_i$, causes facilitation by increasing the probability of transmitter release (Katz and Miledi, 1968; Stanley, 1986; Kamiya and Zucker, 1994; Wu and Saggau, 1994; Atluri and Regehr, 1996; Vyshedskiy et al., 2000; Rozov et al., 2001; Zucker and Regehr, 2002).

Nevertheless, the fundamental steps by which residual $[Ca^{2+}]_i$ induces facilitation are controversial. In the simplest case, residual $[Ca^{2+}]_i$ would increase the $[Ca^{2+}]_i$ signal created by a subsequent AP, leading to enhanced transmitter release. However, it is generally accepted that simple summation of residual $[Ca^{2+}]_i$, which is less than 1 μM for a single AP (Helmchen et al., 1997), is not sufficient to induce significant facilitation. This is because it became evident that the $[Ca^{2+}]_i$ signal driving transmitter release is a microdomain signal in the immediate vicinity of open Ca^{2+} channels (Chad and Eckert, 1984; Simon and Llinás, 1985; Adler et al., 1991; Yamada and Zucker, 1992; Roberts, 1994), with amplitudes often calculated to be 100 μM or more (Simon and Llinás, 1985; Yamada and Zucker, 1992; Roberts, 1994; but see Aharon et al., 1994; Meinrenken et al., 2002). Because of the large difference in the amplitudes of residual and microdomain $[Ca^{2+}]_i$, it has been argued that simple summation of residual $[Ca^{2+}]_i$ to microdomain $[Ca^{2+}]_i$ cannot be effective in causing facilitation (Zucker and Regehr, 2002). Therefore, models for facilitation based on putative high-affinity Ca^{2+} binding sites have been developed (Yamada and Zucker, 1992; Bertram et al., 1996; Atluri and Regehr, 1996; Tang et al., 2000). In one class of model, it is assumed that Ca^{2+} that remains bound to a high-affinity binding site of the secretory trigger causes facilitation (Yamada and Zucker, 1992; Bertram et al., 1996). This "bound Ca^{2+} model" predicts that during facilitation, the Ca^{2+} sensitivity of transmitter release is increased (Bertram et al., 1996). In other models, the strength of facilitation is proportional to the occupancy of a high-affinity Ca^{2+} binding site, which is separate from the Ca^{2+} sensor for vesicle fusion (Atluri and Regehr, 1996; Tang et al., 2000; Dittman et al., 2000; Matveev et al., 2002). This class of models will be termed the "two-sensor model" of facilitation. Both the bound Ca^{2+} model and the two-sensor model for facilitation predict that during facilitation, a virtually unchanged microdomain $[Ca^{2+}]_i$ signal encounters a facilitated release machinery that triggers transmitter release with higher probability, caused by an increased occupancy of a high-affinity Ca^{2+} binding site for facilitation.

It is well known that Ca^{2+} triggers neurotransmitter release in a highly nonlinear fashion, with apparent cooperativities of 3–4 when varying the extracellular (Dodge and Rahamimoff, 1967) or the intracellular Ca^{2+} concentration (Heidelberger et al., 1994; Landò and Zucker, 1994). Recent studies using Ca^{2+} uncaging and Ca^{2+} imaging at the calyx of Held have confirmed a high intracellular Ca^{2+} cooperativity of 4–5 and have shown that the Ca^{2+} sensitivity of transmitter release is unexpectedly high (Bollmann et al., 2000; Schneggenburger and Neher, 2000). Transmitter release rates induced by presynaptic APs were found compatible with brief microdomain $[Ca^{2+}]_i$ transients with peak amplitudes of 10 μM (Bollmann et al., 2000) or 25 μM (Schneggenburger and Neher, 2000). The lower estimates of the microdomain $[Ca^{2+}]_i$, together with the high cooperativity of Ca^{2+} in triggering transmitter release, have prompted us to address the role of $[Ca^{2+}]_i$ summation in synaptic facilitation. Using presynaptic Ca^{2+} uncaging at the calyx of Held to induce transmitter release, we show here that during Ca^{2+}-induced synaptic facilitation, the Ca^{2+} cooperativity and the Ca^{2+} dependence of release kinetics are largely unchanged, implying that facilitation is caused by an increased microdomain $[Ca^{2+}]_i$ signal for transmitter release.

*Correspondence: rschneg@gwdg.de

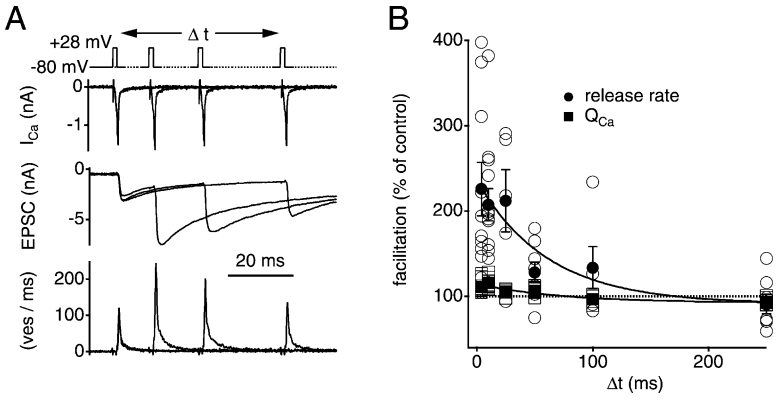

Figure 1. Paired-Pulse Facilitation under Pre- and Postsynaptic Voltage-Clamp at the Calyx of Held

(A) A short (1.2 ms) presynaptic depolarization to +28mV was given as a test stimulus, followed by a second identical pulse after a variable time interval, Δt. Presynaptic Ca^{2+} currents (upper panel), EPSCs from the postsynaptic recording (middle), and transmitter release rates (lower) analyzed from EPSC deconvolution (see Experimental Procedures; and Neher and Sakaba, 2001) are shown.

(B) Plot of individual data points for facilitation (open circles), as calculated from peak transmitter release rates (see Experimental Procedures), and of the relative presynaptic Ca^{2+} current integral (square data points). The average data points for facilitation from n = 7 cells (filled circles) were fitted with an exponential function with time constant of 61 ms.

Results

We studied facilitation at the large nerve terminals of the calyces of Held, which are accessible to patch-clamp recordings (Forsythe, 1994; Borst et al., 1995) and to manipulations of presynaptic $[Ca^{2+}]_i$ by uncaging of Ca^{2+} from photolytic chelators (Bollmann et al., 2000; Schneggenburger and Neher, 2000). We made paired whole-cell voltage-clamp recordings from the pre- and postsynaptic elements of the calyx of Held to MNTB principal cell synapse, and recorded excitatory postsynaptic currents (EPSCs) mediated by AMPA-type glutamate receptors as a measure of transmitter release (Neher and Sakaba, 2001). In a first set of experiments, we used a double-pulse protocol with varying intervals to assess the amplitude and the decay kinetics of facilitation (Figure 1). At the calyx of Held, as at many other synapses, facilitation is observed under conditions of reduced initial transmitter release probability (Borst et al., 1995). We therefore used short AP-like presynaptic voltage-clamp steps in paired pre- and postsynaptic whole-cell recordings, aimed at evoking transmitter release comparable to that observed during afferent fiber stimulation at reduced external Ca^{2+} concentration. The duration of the test pulses was adjusted in a range of 0.8–1.5 ms between different cells, resulting in EPSC amplitudes of 2.1 ± 0.17 nA under control conditions (n = 46 EPSCs in seven cell pairs; Figure 1A). We extracted the transmitter release rates by EPSC deconvolution analysis (Neher and Sakaba, 2001) (Figure 1A, lower panel). This revealed an average peak release rate of 104 ± 8.8 vesicles/ms under control conditions and a release rate integral of 72 ± 7 vesicles, corresponding to 4.5% of the average size of a pool of readily releasable vesicles estimated in separate experiments (see below; Figure 3). Thus, the probability of release from the readily releasable pool was low for control conditions.

When the control depolarizations were followed by identical stimuli at varying time intervals, robust paired-pulse facilitation of EPSCs was observed (Figure 1A). Facilitation was 226% ± 31% of the control release rate at the shortest interstimulus interval of 4 ms, and decayed with a time constant of 61 ms (Figure 1B). At the same time, a slight facilitation of the presynaptic Ca^{2+} current (Borst and Sakmann, 1998; Cuttle et al., 1998; Tsujimoto et al., 2002) was observed (Figure 1B; 111% ± 2% of the control Ca^{2+} current integral), which decayed with time and gave way to a small (93% ± 2%) depression of the Ca^{2+} current integral at an interstimuls interval of 250 ms (Figure 1B). Assuming that there is a power relation between transmitter release and presynaptic Ca^{2+} charge with an exponent of about 3, compatible with previous estimates (Takahashi et al., 1996; Wu et al., 1999), a facilitation of transmitter release to about 140% of control is expected. It is unlikely that postsynaptic factors, such as a use-dependent relief of spermine block of postsynaptic AMPA receptors (Rozov et al., 1998), contributed to facilitation, because endogenous intracellular spermine is rapidly removed from the somatic compartment of MNTB principal cells by whole-cell dialysis (M. Barnes-Davies and I.D. Forsythe, 1996, J. Physiol., abstract). Taken together, in order to explain the observed amount of paired-pulse facilitation (~220% of control; see Figure 1B), a presynaptic mechanism of facilitation downstream of changes in Ca^{2+} current must be present.

We sought to maximize the amount of observable facilitation and to isolate the component of facilitation downstream of changes in Ca^{2+} entry. Since facilitation is a Ca^{2+}-dependent process (see Figures 4 and 7, and Zucker and Regehr [2002] for a review), maximizing facilitation requires to inject more Ca^{2+}. However, increasing the Ca^{2+} influx during AP-like conditioning pulses would lead to a disproportionate increase in transmitter release because of the high cooperativity of Ca^{2+} in inducing transmitter release. The resulting partial vesicle pool depletion and synaptic depression could mask facilitation. Therefore, we induced facilitation by applying prolonged conditioning depolarizations (84 ms; Figure 2A) close to the activation threshold for Ca^{2+} currents. At the end of some of the conditioning depolarizations (called "pre-depolarizations" in what follows), asynchronous transmitter release was apparent (Figure 2A, blue EPSC trace, asterisk), which resulted from the accumulation of presynaptic $[Ca^{2+}]_i$. We varied the amplitudes of the pre-depolarizations (range: −30mV to −22mV between cells) until strong facilitation with little preceding asynchronous release was obtained (see Figure 2A, red EPSC

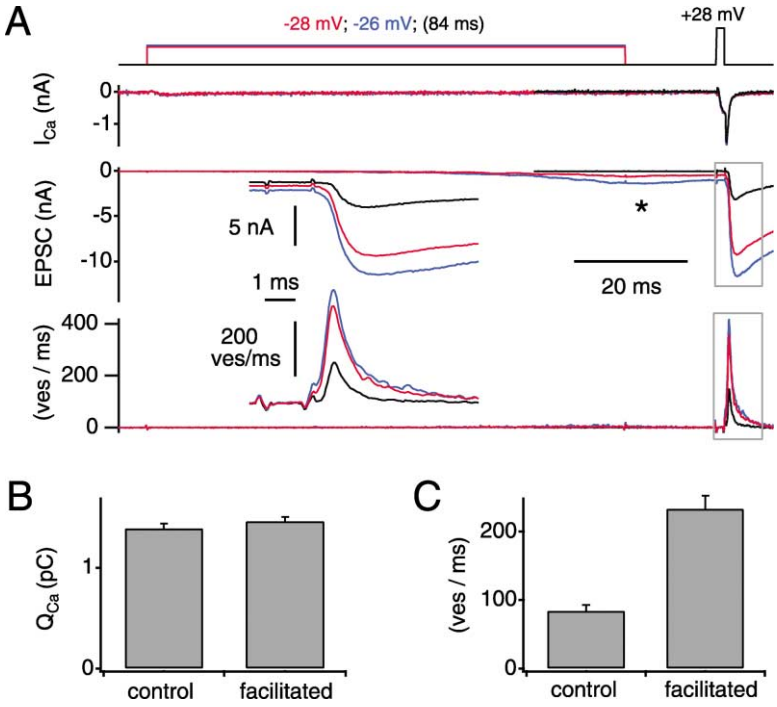

Figure 2. Synaptic Facilitation Induced by Prolonged Presynaptic Depolarizations Close to the Threshold for Ca^{2+} Current Activation

(A) Pre-depolarizations to −28mV and −26mV for 84 ms preceded a 1.5 ms, AP-like test pulse to +28mV. Presynaptic Ca^{2+} current (upper panel), postsynaptic currents (middle), and transmitter release rates (bottom) derived from EPSC deconvolution. Colors identify corresponding traces.

(B) Average charge carried by the Ca^{2+} currents during AP-like stimuli for control (left bar) and facilitated responses (right bar), analyzed for 49 out of 66 trials that showed a relative change of less than 10%.

(C) Peak transmitter release rates for control conditions (left bar) and after induction of facilitation (right bar) for the same trials as analyzed in (B).

trace). In 17 out of 66 paired trials, the Ca^{2+} current integral following pre-depolarizations was changed by more than ±10% with respect to the corresponding control value. To avoid overlap with transmitter release modulation mediated by changes in Ca^{2+} influx, we restricted the analysis to the remaining trials, in which the change in Ca^{2+} current integral was less than ±10%. In this data set, the mean presynaptic Ca^{2+} current integral during the test pulses was virtually unchanged (102% ± 1%, n = 49 trials; Figure 2B). Nevertheless, facilitation of transmitter release during AP-like test pulses was 325% ± 14%, as calculated from the ratio of facilitated release rates over control values (Figure 2C). This shows that facilitation studied under these conditions is mediated almost exclusively by a process downstream of Ca^{2+} entry.

Is it possible that the conditioning pre-depolarizations induced facilitation by increasing the size of a readily releasable vesicle pool? To test this possibility, facilitation was induced and tested similarly as in Figure 2, but a strong, pool-depleting presynaptic depolarization to 0mV for 50 ms was given at the end of the protocol (Figure 3A). This stimulus is expected to deplete the readily releasable pool at the calyx of Held (Sakaba and Neher, 2001; Sun and Wu, 2001). It was found that the EPSC evoked by pool-depleting depolarizations to 0mV was not changed by the conditioning pre-depolarization (Figure 3A, black and red EPSC traces). We analyzed the integrated release rate traces to assess whether facilitation was accompanied by a changed pool size. First, the release rate traces were integrated from the start of the pre-depolarization up to 10 ms after the onset of pool-depleting depolarizations (see Figure 3A, vertical dotted line). The resulting release rate integrals were compared for control protocols and for protocols including pre-depolarizations (Figure 3B, left and right bars). Second, the integration was restricted to the times during which phasic transmitter release was evoked during the test pulses (see Figure 3A, brackets, and Figure 3C). Neither method revealed a significant change in the number of released quanta (see legend to Figure 3 for details). Thus, there was no indication that facilitation was mediated by an increased size of a readily releasable vesicle pool.

We next analyzed the decay of facilitation by varying the interval between pre-depolarizations and AP-like test depolarizations (Figure 4A). An average decay time constant of 114 ± 24 ms (range, 63–195 ms; n = 5 cells) was found, in good agreement with the decay time constant of paired-pulse facilitation studied at other CNS synapses (Wu and Saggau, 1994; Atluri and Regehr, 1996). In another series of experiments (n = 6 cells), we included fura-2FF in the presynaptic patch pipette to measure the decay of the spatially averaged $[Ca^{2+}]_i$ together with the decay of facilitation (Figure 4B). Both decay time constants varied between cells, but the two quantities were correlated (r = 0.86; Figure 4C). Thus, facilitation induced by pre-depolarizations represents an increase in transmitter release probability (Figure 3) and decays with a time constant nearly linearly related to the decay time constant of residual $[Ca^{2+}]_i$ (Figure 4C). These properties are thought to be shared by paired-pulse facilitation observed at other CNS synapses (Wu and Saggau, 1994; Atluri and Regehr, 1996; Rozov et al., 2001; see Zucker and Regehr, 2002, for a review).

We have so far established that pre-depolarizations induce a robust facilitation of transmitter release at the calyx of Held (~3-fold; Figure 2C) that is induced by elevations in presynaptic $[Ca^{2+}]_i$ but that did not result from changes in Ca^{2+} influx during the test pulse (Figures 2B and 2C). We next asked whether facilitation is caused

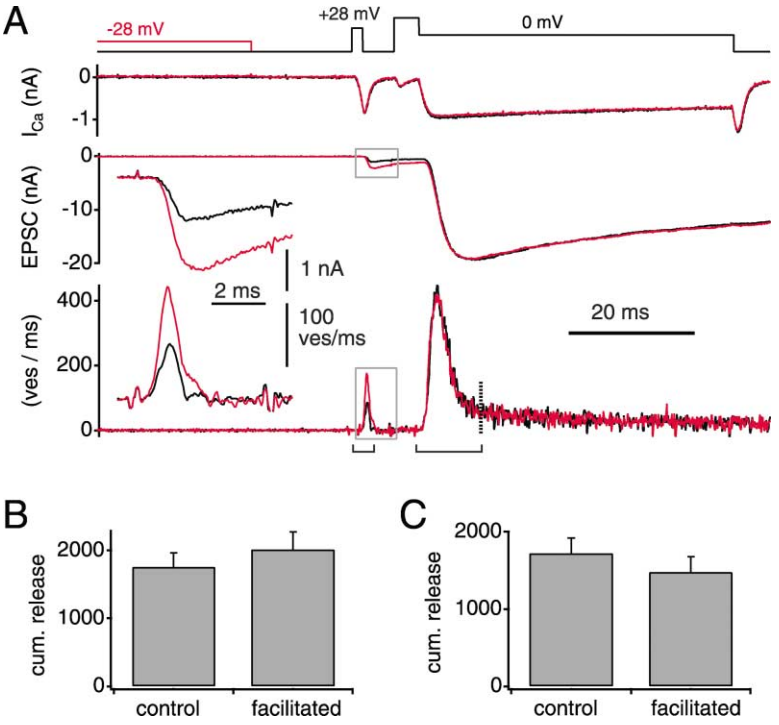

Figure 3. Facilitation Is Not Accompanied by Changes in the Size of the Readily Releasable Vesicle Pool

(A) Facilitation was induced by an 84 ms pre-depolarization to −28mV, similarly as in Figure 2. Following the AP-like test pulse to +28mV, a 50 ms pool-depleting depolarization to 0mV was applied. The response to the pool-depleting stimulus was unchanged for control conditions (black traces) and after induction of facilitation (red traces).

(B and C) Average integrated release rates for controls, and after facilitation, analyzed for n = 9 cell pairs. In (B), release rates were integrated from the beginning of the pre-depolarization up to the end of phasic release triggered by the pool-depleting stimulus (see vertical dotted line in [A]). In (C), release rates were integrated during short time intervals (see brackets in [A]) during which phasic transmitter release occurred. The observed changes in cumulative transmitter release were not statistically significant (p = 0.44 and 0.38 in (B) and (C), respectively).

by a change in the intracellular Ca^{2+} sensitivity of transmitter release. To do so, we induced facilitation by weak pre-depolarizations similar to those in Figures 2–4; however, we now tested transmitter release by Ca^{2+} uncaging (Figure 5). Since Ca^{2+} uncaging leads to a spatially homogenous elevation of $[Ca^{2+}]_i$, fluorescence ratio imaging can be used to measure the $[Ca^{2+}]_i$ relevant for transmitter release (Bollmann et al., 2000; Schneggenburger and Neher, 2000). In the example of Figure 5A (black trace), a control flash elevated presynaptic $[Ca^{2+}]_i$ to 3.8 μM and evoked a slowly rising EPSC of 1.75 nA amplitude. After pre-depolarization, a flash with the same intensity elevated $[Ca^{2+}]_i$ to 6.25 μM and induced a larger and faster rising EPSC (Figure 5A, red trace). From this experiment alone, it is difficult to conclude whether the increased transmitter release following the pre-depolarization was caused by a genuine facilitatory effect of the pre-elevated $[Ca^{2+}]_i$, or simply because the postflash $[Ca^{2+}]_i$ was higher than for the control condition. Therefore, in other trials, we reduced the intensity of the flashes that followed the pre-depolarizations, with the aim of obtaining similar postflash $[Ca^{2+}]_i$ with and without pre-depolarization. In the experiment of Figure 5B, in which we obtained an almost identical postflash $[Ca^{2+}]_i$, the rise time and the amplitude of the EPSCs evoked by Ca^{2+} uncaging were virtually superimposable for control and pre-depolarization. This indicates that the rate and the kinetics of transmitter release are set by the $[Ca^{2+}]_i$ attained after flashes, but not by $[Ca^{2+}]_i$ preceding the flashes.

In an analysis of many such experiments (Figure 6), the peak transmitter release rates obtained from deconvolution analysis of EPSCs (Figure 5, lower panels) and the synaptic delays were plotted as a function of postflash $[Ca^{2+}]_i$. In the resulting dose-response curves, the data for control and following pre-depolarizations overlapped (Figures 6A and 6B, open and closed symbols). For quantitative comparison, the control data points were fitted with a model that assumes cooperative binding of five Ca^{2+} ions preceding vesicle fusion (Schneggenburger and Neher, 2000) (see Figure 6G). We then analyzed for individual cells (n = 13) the change of release rates and synaptic delays induced by pre-depolarizations, relative to fit lines which best described the control data points of a given cell. The resulting values of relative change scattered around unity (Figures 6C and 6D) and were 1.41 ± 0.12 and 0.914 ± 0.05 on average (n = 45 trials) for release rates and synaptic delays, respectively. Plots of the relative change of release rate and delays against the pre-elevated $[Ca^{2+}]_i$ showed no significant correlation (r = 0.085 and −0.355, respectively, n = 41 trials; Figures 6E and 6F). Thus, pre-elevations of $[Ca^{2+}]_i$ do not lead to a systematic increase in the relationship between transmitter release rates and $[Ca^{2+}]_i$.

The experiments in Figures 5 and 6 did not reveal a major change in the Ca^{2+} dependencies of peak transmitter release rates or synaptic delays during facilitation. This excludes models which assume that Ca^{2+} remaining bound at some site of the Ca^{2+} sensor for vesicle fusion mediate facilitation, because these predict an increased Ca^{2+} sensitivity of transmitter release (Bertram et al., 1996). Since facilitation was not accompanied by an obvious increase in the Ca^{2+} sensitivity of transmitter release (Figure 6) nor in the size of the readily releasable vesicle pool (Figure 3), we next assessed whether facilitation can be explained by summation of residual $[Ca^{2+}]_i$ and microdomain $[Ca^{2+}]_i$. For this purpose, we need to know the effectiveness of conditioning $[Ca^{2+}]_i$ elevations in inducing facilitation. Therefore, we measured the $[Ca^{2+}]_i$ dependence of synaptic facilitation by using Ca^{2+} uncaging to pre-elevate $[Ca^{2+}]_i$ and by

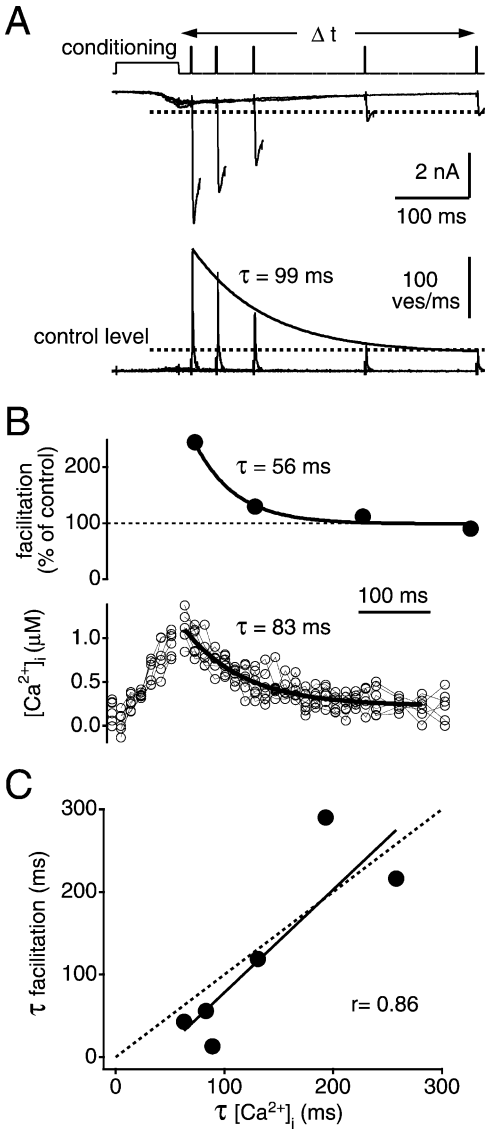

Figure 4. The Decay of Synaptic Facilitation Induced by Pre-Depolarizations Is Rapid and Follows the Decay of Spatially Averaged $[Ca^{2+}]_i$

(A) (Upper panel) Facilitation was induced by pre-depolarizations, and test EPSCs were evoked by AP-like depolarizations at a variable time intervals Δt. For clarity, the response to a second AP-like depolarization following the test pulse is not shown. (Lower panel) Transmitter release rates derived from EPSC deconvolution. The decay of facilitation, measured as the peak transmitter release rate relative to control levels, was fitted with an exponential with time constant of 99 ms. The control amplitudes of EPSCs and transmitter release rates obtained without conditioning pre-depolarizations are indicated by the horizontal dashed lines.

(B) Experiment from a different cell pair. Here, the spatially averaged presynaptic $[Ca^{2+}]_i$ was measured simultaneously with 100 μM fura-2FF. The decay of facilitation (upper panel) and the decay of spatially averaged $[Ca^{2+}]_i$ (lower panel) were fitted with exponential functions.

(C) Relationship between the decay time constants of facilitation and spatially averaged $[Ca^{2+}]_i$ (n = 6 cells). The data fell close to the unity line (dashed line) and were fitted by linear regression (solid line) with a correlation coefficient r of 0.86.

testing transmitter release with AP-like depolarizations (Figure 7). Fura-4F was used as a Ca^{2+} indicator because its relatively high affinity (K_d = 1.1 μM; see Experimental Procedures) is well suited for a quantitative determination of $[Ca^{2+}]_i$ in the relevant submicromolar to low micromolar range. In Figure 7A, a weak flash pre-elevated $[Ca^{2+}]_i$ to 0.8 μM and induced a facilitation of peak release rate of 258% with a virtually unchanged presynaptic Ca^{2+} current (Figure 7A, inset). On average, the Ca^{2+} current integral was 102.1% ± 0.7% of control (n = 61 paired trials in n = 21 cells), showing that facilitation induced by flash-evoked pre-elevations of $[Ca^{2+}]_i$ (Figure 7A) was not the result of Ca^{2+} current facilitation.

With conditioning $[Ca^{2+}]_i$ elevations to different values in n = 10 cells, the apparent $[Ca^{2+}]_i$ dependence of facilitation was measured (Figure 7B, gray data points). In another series of experiments with fura-2FF (n = 11 cells), a similar $[Ca^{2+}]_i$ dependence of facilitation was found (Figure 7B, black data points), although the binned data for $[Ca^{2+}]_i$ above 1 μM showed a slightly smaller facilitation for fura-2FF than for fura-4F (p = 0.13). This difference might be caused by the different Ca^{2+} dissociation constants of the two dyes. The higher-affinity dye fura-4F ($K_d \approx$ 1.1 μM) is more prone to saturation (Adler et al., 1991) during pre-elevation of $[Ca^{2+}]_i$ and will then not be available to buffer incoming Ca^{2+}. This might result in a disinhibition of transmitter release, similar to the previously described effect of "pseudofacilitation" exerted by low concentrations of BAPTA in cortical nerve terminals (Rozov et al., 2001). The $[Ca^{2+}]_i$ dependence of facilitation was confirmed by plotting facilitation as a function of the spatially averaged $[Ca^{2+}]_i$ from the measurements in Figure 4B (Figure 7B, open squares).

Having established the $[Ca^{2+}]_i$ dependence of synaptic facilitation (Figure 7B), we can now ask in a modeling approach whether facilitation is explained by linear $[Ca^{2+}]_i$ summation (Figure 8). For this purpose, we first calculated the inferred microdomain $[Ca^{2+}]_i$ signal compatible with the measured transmitter release rates under control conditions, similarly as shown previously (Bollmann et al., 2000; Schneggenburger and Neher, 2000). This was done by using the kinetic model (Figure 6G) with the fitted parameters from the experiments in Figures 5 and 6 (see Experimental Procedures). In the example of Figure 8A (black traces), a microdomain $[Ca^{2+}]_i$ signal of 9.9 μM amplitude explained the observed control transmitter release rate. If the measured, pre-elevated $[Ca^{2+}]_i$ (1.9 μM in this example) was added to the inferred microdomain $[Ca^{2+}]_i$, and the model of cooperative Ca^{2+} binding and vesicle fusion was driven with the resulting enhanced $[Ca^{2+}]_i$ waveform, a 2.6-fold increase in transmitter release rate was predicted (Figure 8A, dashed blue lines), accounting for 43% of facilitation observed in this example. In a similar analysis of 56 trials in 21 cells, 28.2% ± 4.6% of the observed facilitation was explained by linear summation of the measured pre-elevated $[Ca^{2+}]_i$ to the inferred microdomain $[Ca^{2+}]_i$ signal. In additional simulations (data not shown), we verified that linear $[Ca^{2+}]_i$ summation, together with the assumption of widely distributed peak $[Ca^{2+}]_i$ signals between vesicles (Meinrenken et al., 2002), did not lead to larger predictions of facilitation (see Experimental Procedures).

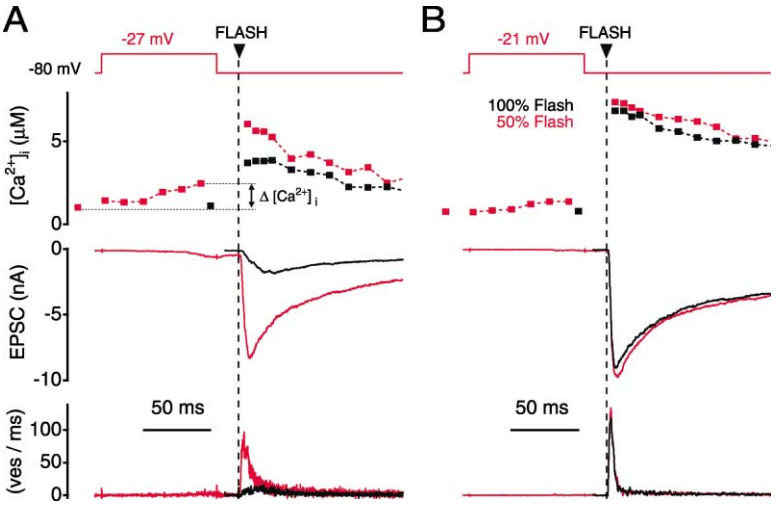

Figure 5. Ca^{2+} Uncaging Shows that Transmitter Release Rate and Release Kinetics Are Determined by Postflash $[Ca^{2+}]_i$ but Not by Pre-Elevated $[Ca^{2+}]_i$

Transmitter release was probed by Ca^{2+} uncaging using flash-photolysis of Ca^{2+}-loaded DM-nitrophen (see Experimental Procedures) with and without pre-depolarizations (red and black traces, respectively). (Upper panel) Presynaptic $[Ca^{2+}]_i$ measured with fura-2FF, (middle) EPSCs in response to presynaptic Ca^{2+} uncaging, and (bottom) transmitter release rates from deconvolution of EPSCs. In (B), the flash intensity after pre-depolarization (red trace) was dimmed to 50%. Note that similar postflash $[Ca^{2+}]_i$ was attained, which evoked EPSCs of similar amplitude and rising phase, irrespective of the pre-elevated $[Ca^{2+}]_i$.

We are now confronted with experimental evidence suggesting, on the one hand, that the Ca^{2+} sensitivity of the release machinery is changed only minimally following pre-elevations of $[Ca^{2+}]_i$ (Figure 6). On the other hand, simple summation of the measured pre-elevated $[Ca^{2+}]_i$ to the inferred microdomain $[Ca^{2+}]_i$ accounts for only about 30% of the observed facilitation (Figures 7B and 8). One possibility to explain the remaining facilitation is to assume that pre-elevation of $[Ca^{2+}]_i$ leads to a more efficient rise in microdomain $[Ca^{2+}]_i$ by a given Ca^{2+} influx. Such an effect is expected to occur by saturation of cellular Ca^{2+} buffer(s) (Neher, 1998; Maeda et al., 1999) during the pre-elevation of $[Ca^{2+}]_i$. We assessed the degree of such a supralinearity in the summation of pre-elevated $[Ca^{2+}]_i$ and microdomain $[Ca^{2+}]_i$ needed to explain facilitation. This was done by scaling

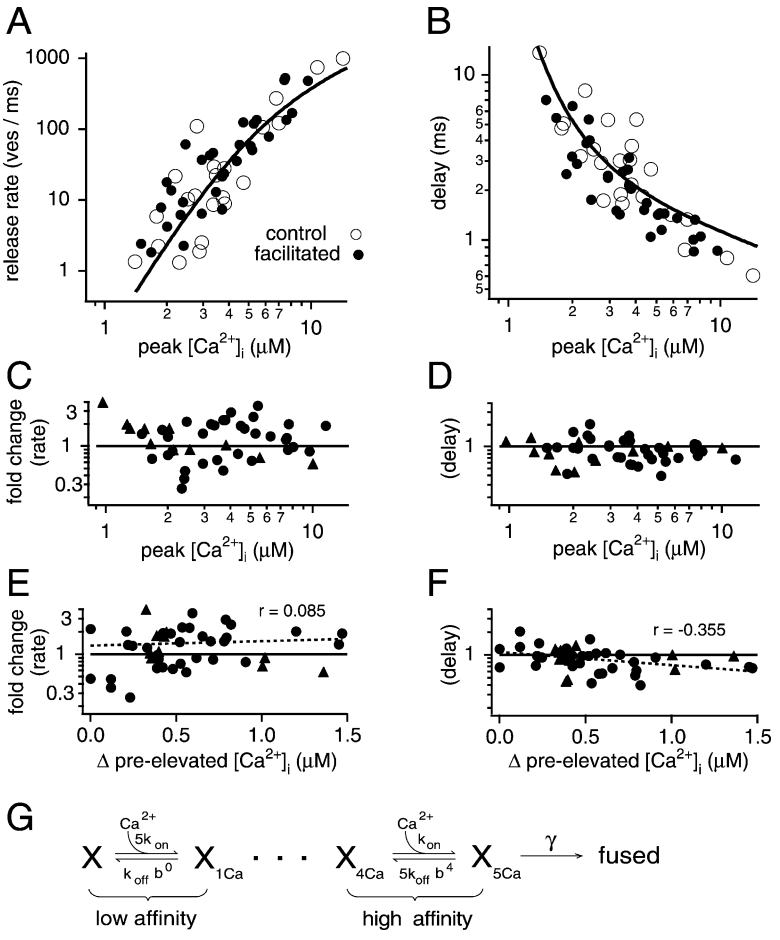

Figure 6. The Intracellular Ca^{2+} Dependence of Transmitter Release Rates and Synaptic Delays Are Largely Unchanged by Pre-Elevations of $[Ca^{2+}]_i$

(A and B) Peak release rates (A) and synaptic delays (B) as a function of peak $[Ca^{2+}]_i$ attained after flashes for controls (open symbols) and after pre-depolarization (closed symbols). Lines are fits of a model of cooperative Ca^{2+} binding and vesicle fusion shown in (G) to the control data points.

(C and D) The change produced by pre-depolarizations in release rate (C) and delay (D), relative to fits of the control data points of a given cell, plotted against the peak $[Ca^{2+}]_i$ after flashes.

(E and F) The change in release rate (E) and delay (F) replotted against the measured, pre-elevated $[Ca^{2+}]_i$ (see Figure 5A). Round and triangular data points in (C) to (F) were obtained with fura-2FF ($n = 13$ cells) and fura-4F ($n = 4$ cells), respectively. Linear regression gave correlation coefficents, r, of 0.085 (E) and −0.355 (F).

(G) The model of cooperative Ca^{2+} binding and vesicle fusion used to fit the control data points in (A) and (B). The following parameters were found by a Simplex fit: $k_{on} = 1.16 \times 10^8$ M^{-1} s^{-1}, $k_{off} = 8430$ s^{-1}, $\gamma = 6960$ s^{-1}. The parameter b was fixed at 0.25. Note that these parameters predict a release rate that is slightly leftward-shifted on the Ca^{2+} axis as compared to previous data (Schneggenburger and Neher, 2000), attributable to slight changes in the Ca^{2+} calibration.

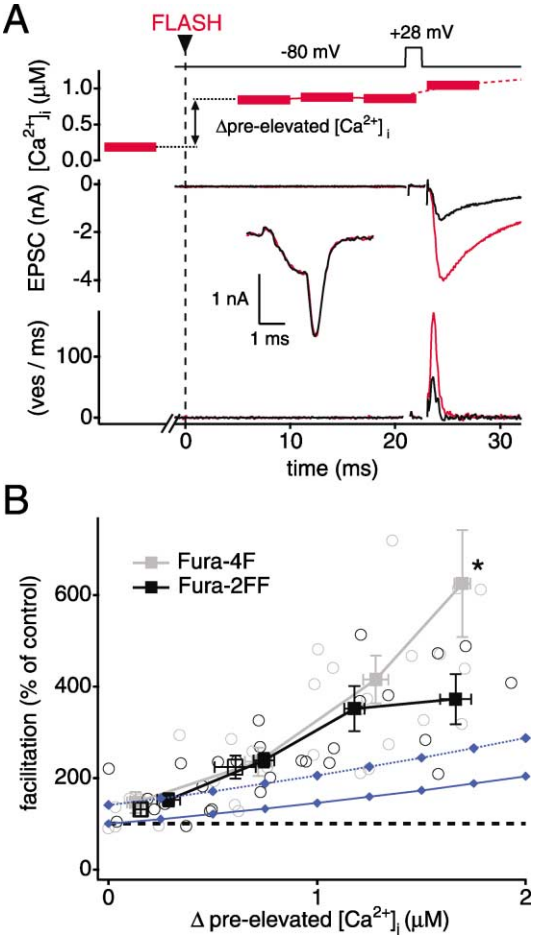

Figure 7. Elevations of $[Ca^{2+}]_i$ by Conditioning Flashes Reveal the Intracellular Ca^{2+} Sensitivity of Synaptic Facilitation

(A) Facilitation was induced by pre-elevating $[Ca^{2+}]_i$ by Ca^{2+} uncaging, and transmitter release was tested with AP-like depolarizations to + 28mV. Pre-elevation of $[Ca^{2+}]_i$ by 0.65 μM (upper panel) induced a 258% facilitation of transmitter release rate (lower panel). Note that the Ca^{2+} currents in response to the test depolarizations were virtually unchanged (superimposed traces in inset).

(B) Facilitation as a function of pre-elevated $[Ca^{2+}]_i$, measured either with fura-2FF (100 μM, black symbols) or with fura-4F (70 or 90 μM; gray symbols). The asterisk indicates a statistically suggestive ($p = 0.13$) difference between the rightmost average data points for fura-4F and fura-2FF (filled symbols). The solid blue line is the prediction for linear summation of $[Ca^{2+}]_i$ (see Experimental Procedures). The dashed blue line was calculated by multiplying the prediction for linear $[Ca^{2+}]_i$ summation with 1.4, thus indicating the possible effect of a slight change in the Ca^{2+} sensitivity of transmitter release (Figure 6E).

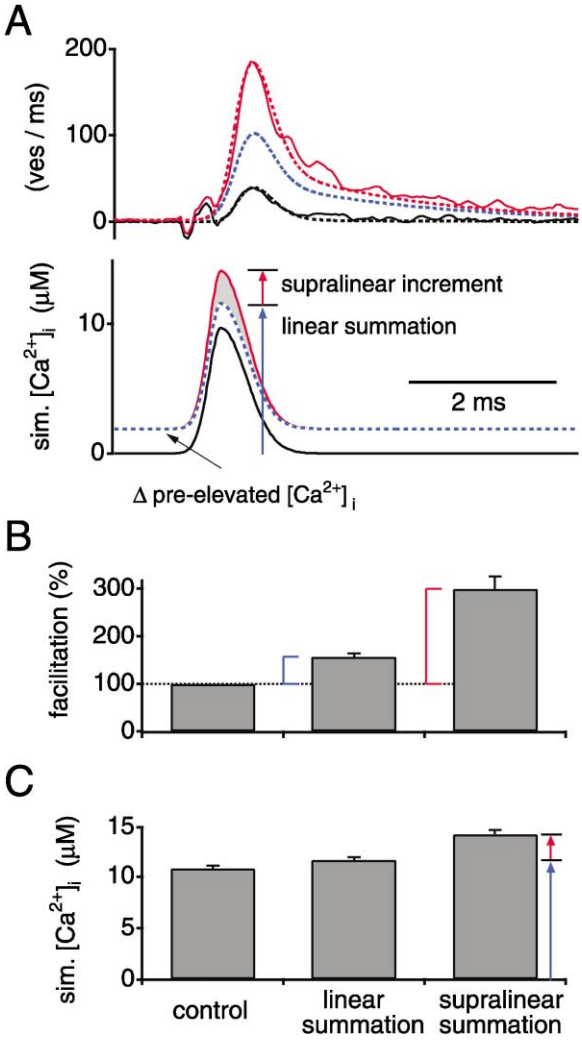

Figure 8. The Contribution of Linear $[Ca^{2+}]_i$ Summation to Facilitation of Transmitter Release at the Calyx of Held

(A) The measured transmitter release rates (upper panel, solid data traces) and the simulated microdomain $[Ca^{2+}]_i$ signals (lower panel) required to explain control and facilitated transmitter release. The predicted transmitter release rates (upper panel, dashed lines) were calculated by driving the model of cooperative Ca^{2+} binding and vesicle fusion (Figure 6G) with the corresponding $[Ca^{2+}]_i$ traces. Adding the measured, pre-elevated $[Ca^{2+}]_i$ of 1.9 μM to the inferred microdomain $[Ca^{2+}]_i$ signal for control release explained about half of the observed facilitation in this example. Assuming that facilitation is mediated entirely by an increased microdomain $[Ca^{2+}]_i$ (see Discussion), the necessary supralinear increment in the microdomain $[Ca^{2+}]_i$ can be assessed (see red traces).

(B and C) Average results of the analysis shown in (A). Facilitation (B) and the peak amplitude of the inferred microdomain $[Ca^{2+}]_i$ signal (C) are shown. Note that linear $[Ca^{2+}]_i$ summation (second bar) explains about 30% of the observed facilitation (compare blue and red brackets in [B]). Supralinear summation of $[Ca^{2+}]_i$, with an increment 22.9% ± 2.3% (see red arrow in [C]; n = 62 paired trials) over the linear $[Ca^{2+}]_i$ sum, was sufficient to fully explain facilitation.

the inferred microdomain $[Ca^{2+}]_i$ signal before adding the measured pre-elevated $[Ca^{2+}]_i$, with the aim of obtaining a prediction that matched the observed transmitter release rates during facilitation (Figure 8A, red traces). The average results of this analysis, obtained in 62 paired trials with fura-2FF and fura-4F (n = 21 cells), are shown in Figure 8B. Linear $[Ca^{2+}]_i$ summation accounted for a facilitation of 156.2% ± 7.5%, which represents 28.2% of the observed facilitation of 299.4% ± 26% (Figure 8B, compare blue and red brackets). An assumed supralinear increment of 22.9% ± 2.3% above the value calculated for the case of linear $[Ca^{2+}]_i$ summation (Figure 8C, red arrow) explained the observed facilitation (Figures 8B and 8C, right bars). Thus, a small degree of supralinearity in the summation of $[Ca^{2+}]_i$ can explain facilitation, because any increase in $[Ca^{2+}]_i$ is amplified by the highly nonlinear Ca^{2+} sens-

ing mechanism for vesicle fusion (Bollmann et al., 2000; Schneggenburger and Neher, 2000). However, we cannot exclude at present that other mechanisms, such as a rapidly equilibrating Ca^{2+} binding site for facilitation (Tang et al., 2000; Matveev et al., 2002) (see Discussion), contribute to the difference between the observed magnitude of facilitation and the prediction based on linear $[Ca^{2+}]_i$ summation.

Discussion

We have investigated the mechanisms of facilitation of transmitter release at the calyx of Held, a large glutamatergic terminal in the auditory pathway. The main finding is that conditioning elevations of $[Ca^{2+}]_i$ in the nerve terminal did not lead to marked changes in the Ca^{2+} dependence of transmitter release rates or synaptic delays (Figure 6), although similar pre-elevations of $[Ca^{2+}]_i$ induced an ~3-fold facilitation of transmitter release evoked by AP-like depolarizations (Figures 2–4). Facilitation was not mediated by an increased size of a readily releasable vesicle pool (Figure 3). We have found that the direct role of $[Ca^{2+}]_i$ summation in inducing synaptic facilitation is larger than previously expected (Zucker and Regehr, 2002), reflecting the moderate amplitude of local (microdomain) Ca^{2+} signals and the unexpectedly high Ca^{2+} sensititivity of vesicle fusion at the calyx of Held (Bollmann et al., 2000; Schneggenburger and Neher, 2000; and see Figure 6). These findings place tight experimental constraints on models for synaptic facilitation.

Facilitation evoked by presynaptic voltage-clamp pulses (Figures 1–4) shared many properties of paired-pulse facilitation studied at other CNS synapses. Thus, facilitation decayed with a time constant in the range of 50–300 ms between different cells (Figures 1 and 4), in good agreement with findings at other excitatory CNS synapses (Wu and Saggau, 1994; Atluri and Regehr, 1996). In combined measurements of the decay of presynaptic $[Ca^{2+}]_i$ and the decay of facilitation (Figures 4B and 4C), we observed a considerable variability of $[Ca^{2+}]_i$ decay time constants between cells. This might be caused by cell-to-cell differences in the Ca^{2+} extrusion rates or, alternatively, in the Ca^{2+} buffering capacity between nerve terminals, since endogeneous Ca^{2+} buffering capacity was shown to influence the decay of spatially averaged $[Ca^{2+}]_i$ (Helmchen et al., 1997). The decay of facilitation, in turn, was correlated with the decay of spatially averaged $[Ca^{2+}]_i$ between different cells (Figure 4C), indicating a causal relation between the two quantities (Zucker and Regehr, 2002). Also, facilitation was not accompanied by an increased size of a readily releasable vesicle pool as estimated by pool-depleting, presynaptic depolarizations (Figure 3). Thus, facilitation induced by presynaptic voltage-clamp steps reflects a transient increase in release probability, similar to that found at many other synapses (see Zucker and Regehr, 2002, for a review).

During synaptic facilitation, the intracellular Ca^{2+} sensitivity of transmitter release rates and synaptic delays were not changed by a major degree, as tested by $[Ca^{2+}]_i$ steps produced by flash-evoked Ca^{2+} uncaging (Figures 5 and 6). This rules out bound Ca^{2+} models for facilitation, which assume that Ca^{2+} remaining bound to a high-affinity site of the Ca^{2+} sensor for vesicle fusion causes facilitation (Yamada and Zucker, 1992; Bertram et al., 1996), because these predict an increased Ca^{2+} sensitivity and/or a reduced synaptic delay during facilitation. On the basis of the experiments in Figures 5 and 6, it might be more difficult to exclude two-sensor models of facilitation (Tang et al., 2000; Matveev et al., 2002) if a high-affinity Ca^{2+} binding site for facilitation equilibrates within the time needed to elevate $[Ca^{2+}]_i$ by a flash (~1 ms; see Experimental Procedures). However, as has been pointed out previously (Tang et al., 2000), such a rapid equilibration implies that the facilitation site must be spatially segregated from the Ca^{2+} sensors for vesicle fusion, because otherwise the facilitation site would be saturated by the rapid rise of local $[Ca^{2+}]_i$ that drives vesicle fusion during an AP. At the calyx of Held, where the local $[Ca^{2+}]_i$ signal for vesicle fusion is created by overlapping domains from several Ca^{2+} channels (Borst and Sakmann, 1996), with estimated diffusional distances in the hundred nanometer range (Meinrenken et al., 2002), it seems unlikely that a maximal distance between the two sites of about 50 nm (the vesicle diameter; Sätzler et al., 2002) will create a sufficiently steep $[Ca^{2+}]$ gradient to protect the facilitation site from saturation. Therefore, facilitation at the calyx of Held is probably not mediated by a rapid facilitation site. It is possible, however, that such a site induces facilitation at other synapses, such as at the crayfish neuromuscular junction (Tang et al., 2000; Matveev et al., 2002).

Another possibility to explain facilitation in the framework of the two-sensor model is to assume that Ca^{2+} binding to the facilitation site lowers an energy barrier for vesicle fusion and thereby increases release probability, as has been suggested for augmentation (Stevens and Wesseling, 1999). However, such a model is unlikely to explain facilitation at the calyx of Held. First, if Ca^{2+} binding to the facilitation site occurs with slow kinetics, then increased release rates at a given post-flash $[Ca^{2+}]_i$ should have been observed during facilitation, opposite to our findings in Figure 6. Second, if Ca^{2+} binding to the facilitation site equilibrated very rapidly, then the two sensors must be spatially separated (Tang et al., 2000), which we regard as an unlikely scenario at the calyx of Held (see above). Also, the relationship between transmitter release rate and $[Ca^{2+}]_i$ can be fitted with models with a high final fusion rate (γ in the scheme of Figure 6G). This indicates that Ca^{2+} binding to the sensor for vesicle fusion, but not the final fusion rate, limits transmitter release under basal conditions. This is corroborated by our finding of a steep dependency of minimal synaptic delay as a function of postflash $[Ca^{2+}]_i$ (Figure 6B) (Schneggenburger and Neher, 2000). Thus, we expect that facilitation is more effectively induced by increasing the fraction of readily releasable vesicles that experience a fully occupied Ca^{2+} sensor for secretion. This, in our view, is brought about by an increased microdomain $[Ca^{2+}]_i$ signal for vesicle fusion.

By using Ca^{2+} uncaging to elevate $[Ca^{2+}]_i$ in a spatially homogeneous manner, we have determined the Ca^{2+} dependence of facilitation (Figure 7). A roughly linear Ca^{2+} dependence, with a slope of ~3-fold facilitation per micromolar pre-elevated $[Ca^{2+}]_i$, was apparent (Figure 7B). Previous studies have found near-linear rela-

tionships between synaptic enhancement and presynaptic $[Ca^{2+}]_i$ measured after spatial equilibration (Swandulla et al., 1991; Delaney and Tank, 1994; Regehr et al., 1994), but these studies investigated longer lasting forms of synaptic enhancement. We used the relationship between facilitation and $[Ca^{2+}]_i$ (Figure 7B) to assess whether linear summation of pre-elevated $[Ca^{2+}]_i$ to the inferred microdomain $[Ca^{2+}]_i$ is sufficient to predict facilitation (Figure 7B, blue line), exploiting the known relationship between $[Ca^{2+}]_i$ and transmitter release at the calyx of Held (Figure 6; and Bollmann et al., 2000; Schneggenburger and Neher, 2000). Linear summation of $[Ca^{2+}]_i$ accounted for about 30% of the observed facilitation (Figure 7B, continuous blue line), consistent with the analysis based on individual trials, in which 28.2% ± 4.6% of the observed facilitation was explained by linear $[Ca^{2+}]_i$ summation (Figure 8B).

We conclude that linear addition of pre-elevated $[Ca^{2+}]_i$ to the microdomain $[Ca^{2+}]_i$ created by the opening of Ca^{2+} channels during a test pulse is not sufficient to explain facilitation. Since the Ca^{2+} sensitivity of transmitter release was largely unchanged during facilitation (Figure 6), we asked which degree of supralinearity in the summation of $[Ca^{2+}]_i$ is required to fully explain facilitation (Figure 8C). This showed that a supralinear increment of 22.9% ± 2.3% over the linear sum of pre-elevated $[Ca^{2+}]_i$ and microdomain $[Ca^{2+}]_i$ was sufficient to explain facilitation (Figures 8B and 8C). From the data presented in Figure 6C, an ~1.4-fold increase in sensitivity of transmitter release during facilitation remains possible, although this increase did not correlate with the amplitude of pre-elevated $[Ca^{2+}]_i$ (Figure 6E). Nevertheless, if mechanisms other than an increase in the microdomain $[Ca^{2+}]_i$ had contributed to facilitation, then the degree of supralinearity in the summation of $[Ca^{2+}]_i$ (Figures 8A and 8C) must be regarded as an upper limit estimate.

Supralinearity in the summation of pre-elevated $[Ca^{2+}]_i$ and microdomain $[Ca^{2+}]_i$ may be caused by the presence of saturable Ca^{2+} buffers (Neher, 1998; Maeda et al., 1999). The relatively low estimates of the microdomain $[Ca^{2+}]_i$ for vesicle fusion at the calyx of Held (10–20 μM) (Figure 6; see also Bollmann et al., 2000; Schneggenburger and Neher, 2000), as well as the partial inhibition of transmitter release by low millimolar concentrations of EGTA (Borst and Sakmann, 1996), suggest an average distance in the hundred nanometer range (Meinrenken et al., 2002) between Ca^{2+} sources and Ca^{2+} sensors. Thus, the microdomain $[Ca^{2+}]_i$ likely represents a buffered Ca^{2+} signal, and the supralinearity in the superposition of pre-elevated and microdomain $[Ca^{2+}]_i$ may be caused by a reduction of such buffering due to partial buffer saturation (Neher, 1998). The spatially averaged Ca^{2+} buffering capacity (or Ca^{2+} binding ratio) is ~40 for the calyx of Held (Helmchen et al., 1997), and it is subject to regulation during early postnatal development (Chuhma et al., 2001). It is not known whether the concentration of Ca^{2+} buffers is enriched close to presynaptic active zones. Diverse Ca^{2+} binding proteins (Baimbridge et al., 1992; Rizo and Südhof, 1998) and metabolites (Naraghi and Neher, 1997) with a wide range of binding kinetics and affinities as well as diffusional mobilities might contribute to Ca^{2+} buffering close to the presynaptic active zone. Therefore, a detailed model of the effects of Ca^{2+} buffer saturation on the amplitude and kinetics of the microdomain Ca^{2+} signal must await a better understanding of the molecular identity, as well as of the binding properties and diffusional mobilities, of the implicated Ca^{2+} buffers.

At some cerebellar and cortical synapses (Atluri and Regehr, 1996; Geiger and Jonas, 2000; Rozov et al., 2001), facilitation of transmitter release is stronger than the ~3-fold facilitation which we have observed at 1 μM $[Ca^{2+}]_i$ (Figure 7B). This might be caused by additional mechanisms contributing to facilitation, such as AP broadening (Geiger and Jonas, 2000) and facilitation of Ca^{2+} currents (Borst and Sakmann, 1998; Cuttle et al., 1998; Tsujimoto et al., 2002), which will increase the Ca^{2+} influx during each AP. Moreover, a synapse-specific increase in the expression of Ca^{2+} binding proteins might enhance synaptic facilitation by causing more Ca^{2+} buffer saturation during trains of stimuli. A Ca^{2+} sensor for vesicle fusion with high cooperativity (Landò and Zucker, 1994; Bollmann et al., 2000; Schneggenburger and Neher, 2000; Fernández-Chacón et al., 2001) and moderately high sensitivity (see Figure 6; and Bollmann et al., 2000; Schneggenburger and Neher, 2000) will effectively translate residual $[Ca^{2+}]_i$ into enhanced transmitter release, aided by supralinear summation of $[Ca^{2+}]_i$ in the microdomain.

Experimental Procedures

Electrophysiology and Slice Preparation

Transverse brainstem slices containing the medial nucleus of the trapezoid body were made, using 8- to 10-day-old Wistar rats. Experiments were done at room temperature (21°C–24°C). The extracellular solution contained 125 mM NaCl, 25 mM $NaHCO_3$, 2.5 mM KCl, 1.25 mM NaH_2PO_4, 1 mM $MgCl_2$, 2 mM $CaCl_2$, 25 mM glucose, 0.4 mM ascorbic acid, 3 mM myo-inositol, and 2 mM Na-pyruvate (pH 7.4 when bubbled with 95% O_2, 5% CO_2). During recordings, 10 mM tetraethylammoniumchloride (TEA-Cl), 50 μM D-2-amino-5-phophonovaleric acid, 0.5 μM tetrodotoxin, 100 μM cyclothiazide, and, in some cases, 1 mM kynurenic acid (Figure 3) were also present. Simultaneous pre- and postsynaptic whole-cell recordings at the calyx of Held to MNTB principal cell synapse were made with two patch-clamp amplifiers (EPC9/2, HEKA Elektronik, Lambrecht, Germany) under visual control in an upright microscope (Zeiss, Oberkochen, Gemany) equipped with gradient contrast, infrared illumination (Luigs and Neumann, Ratingen, Germany).

During recordings, series resistances were electronically compensated up to 85%. Postsynaptic current traces were further corrected off-line for the remaining series resistance error. Transmitter release rates were extracted by deconvolving EPSCs with an idealized mEPSC waveform, incorporating a model of glutamate diffusion to subtract a current component caused by glutamate spill-over (Neher and Sakaba, 2001). Presynaptic current traces are shown after P/4 correction. The pipette (intracellular) solutions contained: 130 mM Cs-Gluconate, 10 mM Cs-HEPES, 20 mM TEA-Cl, 3.3 mM $MgCl_2$, 2 mM Na_2ATP, 0.3 mM Na_2GTP. Cs_2-EGTA (5 mM) was added for postsynaptic recordings. The presynaptic solution for the experiments shown in Figures 1–3 and Figure 4A did not contain added Ca^{2+} buffers. Results are reported as average ± SEM. The Student's t test (two-tailed) was used to assess statistical significance.

Ca^{2+} Uncaging and Ca^{2+} Imaging

For the Ca^{2+} uncaging experiments (Figures 5–8), the presynaptic pipette solution contained: 120 mM Cs-gluconate, 20 mM Cs-HEPES, 20 mM TEA-Cl, 5 mM Na_2ATP, 0.3 mM Na_2GTP, 1 (1.5) mM DM-nitrophen, 0.8 (1.2) mM $CaCl_2$, 0.5 (0.8) mM $MgCl_2$, and either 100 μM fura-2FF or 70–90 μM fura-4F as Ca^{2+} indicators. A flash lamp (Rapp Optoelektronik, Hamburg, Germany) was used to photolyze DM-nitrophen. $[Ca^{2+}]_i$ was measured by exciting fura-2FF

(350/380 nm) or fura-4F (355/380 nm) with a monochromator and imaging the resulting fluorescence with a CCD camera (TILL photonics, Gräfelfing, Germany). Pixel binning was 8 × 15, allowing short (5 ms) exposure times for each image. $[Ca^{2+}]_i$ was calculated from background-corrected fluorescence ratios R as (Grynkiewicz et al., 1985):

$$[Ca^{2+}]_i = K_{eff} \cdot \frac{R - R_{min}}{R_{max} - R} \quad (1)$$

The calibration constants R_{min}, R_{max}, and K_{eff} were obtained as follows. First, the dissociation constants (K_d) for fura-2 FF and fura-4F were determined by measuring fluorescence spectra of buffered (DPTA or HEDTA) calibration solutions in small glass cuvettes (100 μm path length; VitroCom, New Jersey), revealing K_d values of 1.1 and 10 μM for fura-4F and fura-2FF, respectively. The limiting ratios at low $[Ca^{2+}]$ (R_{min}; 10 mM EGTA), at high $[Ca^{2+}]$ (R_{max}; 10 mM $CaCl_2$), and an intermediate ratio R_{int} at $[Ca^{2+}]$ close to the K_d of the respective dye were next measured in glass cuvettes, and K_{eff} was calculated after rearranging Equation 1. The calibration constants were corrected (Heinemann et al., 1994) for the effect of photolysis of DM-nitrophen on the fluorescent properties of the indicators (Zucker, 1992). The values for R_{min} (10 mM EGTA) and R_{int} were confirmed in whole-cell measurements of calyces (n = 4 each) by using strong Ca^{2+} buffering (10 mM EGTA, no added $CaCl_2$ for R_{min}; 80 mM DPTA, 10 mM $CaCl_2$ for R_{int} at 10 μM).

Data Analysis

Facilitation was calculated from the ratio of peak transmitter release rates obtained from EPSC deconvolution, according to (facilitated peak release rate/control peak release rate) · 100 (%). For fitting the data in Figures 6A and 6B with a model of cooperative Ca^{2+} binding and vesicle fusion (Figure 6G), we first calculated numerically the expected rise in $[Ca^{2+}]_i$ after a flash, using the measured time course of the flash lamp (1.1 ms half-width) and the kinetics of the implied Ca^{2+} and Mg^{2+} buffers. The resulting waveform had a 10%–90% rise time of 0.95 ms (see Discussion) and showed no appreciable decay following its peak (Figure 3D of Schneggenburger and Neher, 2000). For the fit of the data in Figures 6A and 6B, this $[Ca^{2+}]_i$ waveform was used to drive the kinetic scheme of Figure 6G for a range of peak $[Ca^{2+}]$ amplitudes. We assumed that there were 1800 vesicles in the readily releasable pool, a number similar to the one determined experimentally (Figures 3B and 3C). To account for vesicles that were released during the induction of facilitation, the release rates observed after pre-depolarizations (Figure 6A, closed symbols) were increased by a factor $1 + N_{pre}$/pool size. The resulting correction was small (<1.1), since in most cases the number of pre-released vesicles (N_{pre}) was less than 100. Delays (Figure 6B) are given as the time between the trigger for the flash lamp and the time at which five quanta were released in integrated release rate traces.

Calculations of Linear and Supralinear $[Ca^{2+}]_i$ Summation

The analysis in Figure 8 started by calculating the inferred microdomain $[Ca^{2+}]_i$ signal for transmitter release (Bollmann et al., 2000; Schneggenburger and Neher, 2000) compatible with the experimentally determined Ca^{2+} sensitivity of release (Figure 6). In this modeling approach, we first created waveforms of microdomain $[Ca^{2+}]_i$ by combining two gaussian functions with different half-widths at their peaks (see black curve in Figure 8A, lower panel). These waveforms were used to drive the model of cooperative Ca^{2+} binding and vesicle fusion (Figure 6G), using the model parameters k_{on}, k_{off}, γ and b obtained from fits to experimental data (Figures 6A and 6B). The amplitude, rise time, and decay time of the $[Ca^{2+}]_i$ waveform were varied until the predicted transmitter release rate matched the measured release rate under control conditions (Figure 8A, upper panel, dashed black trace superimposed over the data trace). The predictions for linear and supralinear $[Ca^{2+}]_i$ summation (Figure 8A, dashed blue and red lines, respectively) were obtained as described in the Results section.

For the calculations in Figure 7B, we used an inferred microdomain $[Ca^{2+}]_i$ waveform similar to that shown in Figure 8A (lower panel, black trace). The half-width and the amplitude were set to 0.8 ms and 11.68 μM, respectively, matched to predict the average control release rate in the experiments of Figure 7A (n = 34 trials with fura-2FF). We simulated facilitation expected from linear $[Ca^{2+}]_i$ summation (Figure 7B, blue line) by driving the model of Figure 6G with the sum of pre-elevated $[Ca^{2+}]_i$ and the inferred microdomain $[Ca^{2+}]_i$ waveform. This treatment assumes that all vesicles in the readily releasable pool experience an identical microdomain $[Ca^{2+}]_i$ signal. It has been suggested, however, that variable distances between Ca^{2+} channels and vesicles can lead to a wide distribution of microdomain $[Ca^{2+}]_i$ signals between vesicles (Meinrenken et al., 2002). In additional simulations (data not shown), we therefore tested the influence of widely distributed peak microdomain $[Ca^{2+}]_i$ signals on the predicted magnitude of facilitation. A standard waveform of inferred microdomain $[Ca^{2+}]_i$ (see Figure 8A, lower panel, black trace) was scaled to different peak values and distributed according to gaussian distributions, and the weighted average release rates were calculated. The mean of the distribution of peak $[Ca^{2+}]_i$ values was adjusted so that similar control responses were obtained. These simulations, using a wide range of coefficients of variations (0.1–0.5), showed that facilitation was ~10% *smaller* than predicted by the simple model of linear $[Ca^{2+}]_i$ summation. Thus, variable distances between Ca^{2+} channels and vesicles cannot explain our observation that facilitation is larger than predicted by a model of linear $[Ca^{2+}]_i$ summation (Figure 8).

Acknowledgments

We thank Takeshi Sakaba for comments on the manuscript and for fruitful discussions. This work was supported by grants from the Deutsche Forschungsgemeinschaft (SFB-406, Schn 451/4-1) and by a Heisenberg Fellowship to R.S.

Received: December 2, 2002
Revised: January 16, 2003

References

Adler, E.M., Augustine, G.J., Duffy, S.N., and Charlton, M.P. (1991). Alien intracellular calcium chelators attenuate neurotransmitter release at the squid giant synapse. J. Neurosci. *11*, 1496–1507.

Aharon, S., Parnas, H., and Parnas, I. (1994). The magnitude and significance of Ca^{2+} domains for release of neurotransmitter. Bull. Math. Biol. *56*, 1095–1119.

Atluri, P.P., and Regehr, W.G. (1996). Determinants of the time course of facilitation at the granule cell to purkinje cell synapse. J. Neurosci. *16*, 5661–5671.

Baimbridge, K.G., Celio, M.R., and Rogers, J.H. (1992). Calcium-binding proteins in the nervous system. Trends Neurosci. *15*, 303–308.

Bertram, R., Sherman, A., and Stanley, E.F. (1996). Single-domain/bound calcium hypothesis of transmitter release and facilitation. J. Neurophysiol. *75*, 1919–1931.

Bollmann, J., Sakmann, B., and Borst, J. (2000). Calcium sensitivity of glutamate release in a calyx-type terminal. Science *289*, 953–957.

Borst, J.G.G., and Sakmann, B. (1996). Calcium influx and transmitter release in a fast CNS synapse. Nature *383*, 431–434.

Borst, J.G.G., and Sakmann, B. (1998). Facilitation of presynaptic calcium currents in the rat brainstem. J. Physiol. *513*, 149–155.

Borst, J.G.G., Helmchen, F., and Sakmann, B. (1995). Pre- and postsynaptic whole-cell recordings in the medial nucleus of the trapezoid body of the rat. J. Physiol. *489*, 825–840.

Chad, J.E., and Eckert, R. (1984). Calcium domains associated with individual channels can account for anomalous voltage relations of Ca-dependent responses. Biophys. J. *45*, 993–999.

Chuhma, N., Koyano, K., and Ohmori, H. (2001). Synchronisation of neurotransmitter release during postnatal development in a calyceal presynaptic terminal of rat. J. Physiol. *530*, 93–104.

Cuttle, M.F., Tsujimoto, T., Forsythe, I.D., and Takahashi, T. (1998). Facilitation of the presynaptic calcium current at an auditory synapse in rat brainstem. J. Physiol. *512*, 723–729.

Delaney, K.R., and Tank, D.W. (1994). A quantitative measurement

of the dependence of short-term synaptic enhancement on presynaptic residual calcium. J. Neurosci. *14*, 5885–5902.

Dittman, J.S., Kreitzer, A.C., and Regehr, W.G. (2000). Interplay between facilitation, depression, and residual calcium at three presynaptic terminals. J. Neurosci. *20*, 1374–1385.

Dodge, F.A., and Rahamimoff, R. (1967). Co-operative action of calcium ions in transmitter release at the neuromuscular junction. J. Physiol. *193*, 419–432.

Fernández-Chacón, R., Konigstorfer, A., Gerber, S.H., Garcia, J., Matos, M.F., Stevens, C.F., Brose, N., Rizo, J., Rosenmund, C., and Sudhof, T.C. (2001). Synaptotagmin I functions as a calcium regulator of release probability. Nature *410*, 41–49.

Forsythe, I.D. (1994). Direct patch recording from identified presynaptic terminals mediating glutamatergic EPSCs in the rat CNS, *in vitro*. J. Physiol. *479*, 381–387.

Geiger, J.R., and Jonas, P. (2000). Dynamic control of presynaptic Ca^{2+} inflow by fast-inactivating K^{+} channels in hippocampal mossy fiber boutons. Neuron *28*, 927–939.

Grynkiewicz, G., Poenie, M., and Tsien, R. (1985). A new generation of Ca^{2+} indicators with greatly improved fluorescence properties. J. Biol. Chem. *260*, 3440–3450.

Heidelberger, R., Heinemann, C., Neher, E., and Matthews, G. (1994). Calcium dependence of the rate of exocytosis in a synaptic terminal. Nature *371*, 513–515.

Heinemann, C., Chow, R.H., Neher, E., and Zucker, R.S. (1994). Kinetics of the secretory response in bovine chromaffin cells following flash photolysis of caged Ca^{2+}. Biophys. J. *67*, 2546–2557.

Helmchen, F., Borst, J.G.G., and Sakmann, B. (1997). Calcium dynamics associated with a single action potential in a CNS presynaptic terminal. Biophys. J. *72*, 1458–1471.

Kamiya, H., and Zucker, R.S. (1994). Residual Ca^{2+} and short-term synaptic plasticity. Nature *371*, 603–606.

Katz, B., and Miledi, R. (1968). The role of calcium in neuromuscular facilitation. J. Physiol. *195*, 481–492.

Landò, L., and Zucker, R.S. (1994). Ca^{2+} cooperativity in neurosecretion measured using photolabile Ca^{2+} chelators. J. Neurophysiol. *72*, 825–830.

Maeda, H., Ellis-Davies, G.C.R., Ito, K., Miyashita, Y., and Kasai, H. (1999). Supralinear Ca^{2+} signaling by cooperative and mobile Ca^{2+} buffering in Purkinje neurons. Neuron *24*, 989–1002.

Matveev, V., Sherman, A., and Zucker, R.S. (2002). New and corrected simulations of synaptic facilitation. Biophys. J. *83*, 1368–1373.

Meinrenken, C., Borst, J.G.G., and Sakmann, B. (2002). Calcium secretion coupling at calyx of Held governed by nonuniform channel-vesicle topography. J. Neurosci. *22*, 1648–1667.

Naraghi, M., and Neher, E. (1997). Linearized buffered Ca^{2+} diffusion in microdomains and its implications for calculation of $[Ca^{2+}]$ at the mouth of a calcium channel. J. Neurosci. *17*, 6961–6973.

Neher, E. (1998). Usefulness and limitations of linear approximations to the understanding of Ca^{++} signals. Cell Calcium *24*, 345–357.

Neher, E., and Sakaba, T. (2001). Combining deconvolution and noise analysis for the estimation of transmitter release rates at the calyx of Held. J. Neurosci. *21*, 444–461.

Regehr, W.G., Delaney, K.R., and Tank, D.W. (1994). The role of presynaptic calcium in short-term enhancement at the hippocampal mossy fiber synapse. J. Neurosci. *14*, 523–537.

Rizo, J., and Südhof, T.C. (1998). C2-domains, structure and function of a universal Ca^{2+}-binding domain. J. Biol. Chem. *273*, 15879–15882.

Roberts, W.M. (1994). Localization of calcium signals by a mobile calcium buffer in frog saccular hair cells. J. Neurosci. *14*, 3246–3262.

Rozov, A., Zilberter, Y., Wollmuth, L.P., and Burnashev, N. (1998). Facilitation of currents through rat Ca^{2+}-permeable AMPA receptor channels by activity-dependent relief from polyamine block. J. Physiol. *511*, 361–377.

Rozov, A., Burnashev, N., Sakmann, B., and Neher, E. (2001). Transmitter release modulation by intracellular Ca^{2+} buffers in facilitating and depressing nerve terminals of pyramindal cells in layer 2/3 of the rat neocortex indicates a target cell-specific difference in presynaptic calcium dynamics. J. Physiol. *531*, 807–826.

Sakaba, T., and Neher, E. (2001). Calmodulin mediates rapid recruitment of fast-releasing synaptic vesicles at a calyx-type synapse. Neuron *32*, 1119–1131.

Sätzler, K., Söhl, L.F., Bollmann, J.H., Borst, J.G.G., Frotscher, M., Sakmann, B., and Lübke, J.H.R. (2002). Three-dimensional reconstruction of a calyx of Held and its postsynaptic principal neuron in the medial nucleus of the trapezoid body. J. Neurosci. *22*, 10567–10579.

Schneggenburger, R., and Neher, E. (2000). Intracellular calcium dependence of transmitter release rates at a fast central synapse. Nature *406*, 889–893.

Simon, S.M., and Llinás, R.R. (1985). Compartmentalization of the submembrane calcium activity during calcium influx and its significance in transmitter release. Biophys. J. *48*, 485–498.

Stanley, E.F. (1986). Decline in calcium cooperativity as the basis of facilitation at the squid giant synapse. J. Neurosci. *6*, 782–789.

Stevens, C.F., and Wesseling, J.F. (1999). Augmentation is a potentiation of the exocytotic process. Neuron *22*, 139–146.

Sun, J.-Y., and Wu, L.-G. (2001). Fast kinetics of exocytosis revealed by simultaneous measurements of presynaptic capacitance and postsynaptic currents at a central synapse. Neuron *30*, 171–182.

Swandulla, D., Hans, M., Zipser, K., and Augustine, G.J. (1991). Role of residual calcium in synaptic depression and posttetanic potentiation: fast and slow calcium signaling in nerve terminals. Neuron *7*, 915–926.

Takahashi, T., Forsythe, I.D., Tsujimoto, T., Barnes-Davies, M., and Onodera, K. (1996). Presynaptic calcium current modulation by metabotropic glutamate receptor. Science *274*, 594–597.

Tang, Y., Schlumpberger, T., Kim, T., Lueker, M., and Zucker, R.S. (2000). Effects of mobile buffers on facilitation: experimental and computational studies. Biophys. J. *78*, 2735–2751.

Tsujimoto, T., Jeromin, A., Saitoh, N., Roder, J.C., and Takahashi, T. (2002). Neuronal calcium sensor 1 and activity-dependent facilitation of P/Q-type calcium currents at presynaptic nerve terminals. Science *295*, 2276–2279.

Vyshedskiy, A., Allana, T., and Lin, J.-W. (2000). Analysis of presynaptic Ca^{2+} influx and transmitter release kinetics during facilitation at the inhibitor of the crayfish neuromuscular junction. J. Neurosci. *20*, 6326–6332.

Wu, L.G., and Saggau, P. (1994). Presynaptic calcium is increased during normal synaptic transmission and paired-pulse facilitation, but not in long-term potentiation in area CA1 of hippocampus. J. Neurosci. *14*, 645–654.

Wu, L.G., Westenbroek, R.E., Borst, J.G.G., Catterall, W.A., and Sakmann, B. (1999). Calcium channel types with distinct presynaptic localization couple differentially to transmitter release in single calyx-type synapses. J. Neurosci. *19*, 726–736.

Yamada, W.M., and Zucker, R.S. (1992). Time course of transmitter release calculated from simulations of a calcium diffusion model. Biophys. J. *61*, 671–682.

Zucker, R.S. (1992). Effects of photolabile calcium chelators on fluorescent calcium indicators. Cell Calcium *13*, 29–40.

Zucker, R.S., and Regehr, W.G. (2002). Short-term synaptic plasticity. Annu. Rev. Physiol. *64*, 355–405.